Chest Loading Reduction with an Additional Load Limiter in the Lower Inboard Diagonal belt: a Simulation Study with the SAFER Human Body Model and THOR on a Rear Seat

Anurag Soni, Stefan Schilling, Jan Faust and Burkhard Eickhoff

Abstract In frontal crashes, rear-seat occupants are protected by belt systems. Force transfer to the chest can be limited with retractor load limiters to reduce the risk of thoracic injuries, but this comes at the expense of larger forward excursion of the occupant, increasing the risk of injuries from interior contact. The objective of this study was to investigate whether an additional load limiter at the lower diagonal belt portion (B4LL) would influence the belt force distribution and, consequently, reduce chest loading without substantially affecting the forward excursion. A frontal crash at 56 kph was simulated with the mid-sized male version of the SAFER Human Body Model and THOR on a generic rear seat. The reference belt system consisted of a retractor model, including a pretensioner and a load limiter (at 5 kN), and a locking tongue. The added B4LL was modeled using a spring with a constant force level that varied from 3 kN to 5 kN. The B4LL effectively reduced forces in the lower area of the diagonal belt – in contrast to the retractor load limiter, which did not substantially affect these forces. The B4LL reduced the chest injury measures in both the occupant models without substantially increasing the forward displacement.

Keywords Occupant, Rib Fracture, Safety, Seatbelt, Thorax.

I. INTRODUCTION

Seat belts are the most important occupant protection device in a vehicle crash [1]. Advanced belt systems, i.e. a belt system that includes a retractor with pretensioner (RP) and load limiter (RLL), have improved the efficiency of seat belts in preventing fatalities and injuries in vehicle crashes [2-3]. The pretensioner improves occupant-to-belt coupling by retracting the seat belt (pretensioner stroke) and removing excess slack almost instantly after sensing a crash. The load limiter controls the force in the seat belt, allowing the occupant to move forward in a crash and preventing the shoulder belt from exerting excessive force on the occupant's chest. Therefore, in a frontal crash, the required force level at the load limiter must balance the force on the chest against the occupant forward excursion. The higher the load limiter level, the less excursion but the higher the chest injury risk; conversely, the lower the load limiter level, the lower the risk of chest injuries but the higher the head-to-vehicle interior contact (injury) risk owing to increased excursion. In the absence of any supplementary restraint systems available in rear seats, such as frontal airbags, load limiters alone must address the challenge of reducing chest deflection without allowing excessive head excursion.

Several field studies have indicated that the most common source of injury to restrained rear-seat adult occupants in frontal crashes is the shoulder belt, with 76% of AIS3+ injuries in occupants over the age of 13 years occurring in the thorax [4-6]. These studies pointed out that the restraint strategies that reduce loading to the chest, such as belt load limiters, could be beneficial for the rear-seat environment, but there may be potential tradeoffs with increased head excursion [7].

A few studies [8-11] have explored the sensitivities of retractor pretensioner strokes and load limiter levels for rear-seats occupants on the trade-offs between chest deflection and forward excursion. All of these studies concluded that it was possible to reduce chest deflection with advanced belt systems, but only at the expense of forward excursion.

A pre-tensioned, load-limiting rear seat-belt system reduced chest deflection measured in a Hybrid III 50th percentile male (H350) dummy compared to a standard 3-point seat belt in 50 kph frontal sled tests [9]. There was c. 15% reduction in the chest deflection with a reduction of load limiter level from 10 kN to 7 kN for an increase of 50 mm in the head forward excursion. However, with a further reduction of the force level to 5 kN, head forward excursion increased substantially (another 140 mm, i.e. to 540 mm), with a small reduction of only

Dr A. Soni (e-mail: anurag.soni@autoliv.com; tel: +49-41217975620), S. Schilling, J. Faust and Dr B. Eickhoff work at Autoliv North Germany.

5% in chest deflection. It was noted that optimal load limiter level would depend upon the occupant size, crash severity and the available space in the rear-seat compartment for a given car [9].

Many different combinations of rear-seat pre-tensioner and load limiter characteristics exist that may reduce chest deflection with the H350 and Hybrid III 5th percentile female (H305) dummies [10]. It was demonstrated that with a reduction in load limiter level from 10 kN to 5 kN, H350 chest deflection reduced by 20% to 25%, but head forward excursion increased by 90 mm to 105 mm, whereas H305 had hardly any change in chest deflection and head forward excursion [10].

Potential benefits and trade-offs of a more advanced belt system were also investigated [11]. Frontal impact sled tests at two speeds (48 kph and 29 kph) with four dummies (the Hybrid III six-year-old (in a booster seat, H3-6YO), the H305, the H350, and the THOR-NT) in the rear seat were conducted. A dual stage progressive load limiter was employed that had two levels of force limiting (initial lower level at 3 kN and then a higher level at 4.5 kN) instead of constant load limiters used in the previous studies. Such a belt system was thought to better control excursion for the wide range of occupant sizes, ranging from small children to large adults. The advanced belt system did indeed limit the forward excursion for two larger dummies (both H350 and THOR-NT) and reduced the chest deflection for all sizes of H3 dummies (H3-6YO, H305 and H350) compared to standard belt system. Interestingly, however, there was no significant decrease in chest deflection in THOR-NT dummy. It was argued that chest deflection in THOR-NT was somehow linked to the force in the lower shoulder-belt portion, which did not change between the two belt systems. Only the upper shoulder-belt force reduced with advanced restraints compared to the standard belt. On the other hand, belt force reduced in both upper and lower shoulder-belt portions with all the H3 dummies with the advanced system [11].

Similar observations with the THOR were reported again [12]. A variety of restraint systems – a standard 3-point belt; advanced-belt only (3-point belts with a pretensioner, load limiter, dynamic locking tongue, and 4-point belts); and advanced-belt with airbag concepts (inflatable belts, Bag in Roof (BiR), and Self Conforming Rear seat Air Bag (SCaRAB)) – were evaluated in three series of sled tests with four dummies (the H3-6YO, the H305, the H3 95th percentile, and the THOR) and two crash pulses. The advanced restraint systems substantially reduced almost all the injury measures for different sizes of H3 dummies. However, none of those restraints reduced the chest deflections for the THOR because the maximal chest deflection of the THOR always occurred at the lower chest location, close to the buckle, which was found to be insensitive to the retractor load limiter level. It was cautiously noted that lowering the shoulder-belt load limit was not effective in reducing the maximal chest deflection of THOR [12].

All the above-mentioned studies focused on reducing the force on the chest by controlling the load limiter force level in the retractor, with an understanding that force in the entire diagonal belt can be controlled by the force level defined at the retractor load limiter. This assumption remained valid with H350 but differed with THOR, where belt force in the lower shoulder-belt portion remained unaffected with the change in retractor load limiter level. This implies that reducing the force in the upper shoulder-belt portion is not sufficient. The force in the lower shoulder belt also needs to be reduced to an adequate level to produce a consistent reduction in chest loading. In fact, the locking tongue was developed with the same intention of lowering the higher forces in the inboard belt, as frequently seen in standard 3-point belt systems, and it showed significant improvements in reducing the chest deflection [13]. The split buckle tongue [14-15] was also conceptualized with an intention to reduce the restraining force on the chest by distributing more forces on anatomical parts that can withstand higher force (i.e. clavicle and pelvis).

The argument can be further supported by the results of a recent field study [16] which evaluated the patterns of rib fractures in adult occupants in real-world frontal crashes. It was found that rib fractures were mainly located near the path of the shoulder belt for belted occupants, with belt involved as primary component, and that the majority of fractures (65%) occurred on the buckle side of the thorax. Knowing that force in the diagonal belt is the dominant factor for the chest loading and that the chest deflection correlates to forces in both upper and lower portions of the diagonal belt, the higher fractures in inboard ribs could reasonably be attributed to the higher forces in the inboard portion of the diagonal belt.

All these studies suggest the need to reduce the belt force in the lower inboard diagonal belt. Therefore, the objective of this study was to investigate if an additional load limiter at the lower diagonal belt portion (B4LL) could reduce the belt force, and thereby the chest loading, without substantially affecting the forward excursion for average 50th percentile male occupants on rear seats.

II. METHODS

Computational Modeling

A finite element (FE) simulation model of generic rear-seat environment was created in LS-Dyna solver. It was validated by means of Body-In-White (BIW) sled tests conducted with the H350 dummy. To compare the simulation results to physical test results, CORA rating was performed using META post processor (ver. 20.1.1) according to ISO 18571 [17]. The CORA rating scale ranges from 0.0 (no correlation between curves) to 1.0 (excellent correlation between curves). The response of the simulation model matched adequately to the test results and achieved an average CORA rating of 0.7 based on head, chest and pelvis resultant accelerations and chest deflection. A summary of the validation results is given in Appendix A1. The validated rear-seat model was utilized in the current investigation.

The mid-sized male model of the SAFER Human Body Model (SAFER HBM) (version 9) [18] and 50th percentile male model of Test Device for Human Occupant Restraint (THOR) (CAE version 1.8.1, from Humanetics Innovative Solutions, Inc) were positioned in the upright posture in the rear-seat model (as shown in Fig. 1(a)) using pre-simulation method in PRIMER. The H-point location and joint angles were adapted from the H350 dummy model in the generic rear-seat environment. Figure 1(b) shows the final position of SAFER HBM and THOR overlaid on H350. The belt was routed using seat-belt routing tool in PRIMER. The belt path was defined such that the belt centre line passed over the mid-sternum locations of the respective occupant models whereas positions of belt anchorages were taken from the original model (positions given in Appendix A1). The belt was modelled with seat-belt material (i.e. *MAT_SEATBELT). Automatic surface to surface contact were defined between occupant model to seatbelt and seat structures (rear seat, floor, and portion of front seat). A full-frontal impact at 56 kph was simulated with LS-Dyna solver version mpp971_s_R9.3.1_140922 with 16 CPUs. The crash pulse is shown in Fig. 2.

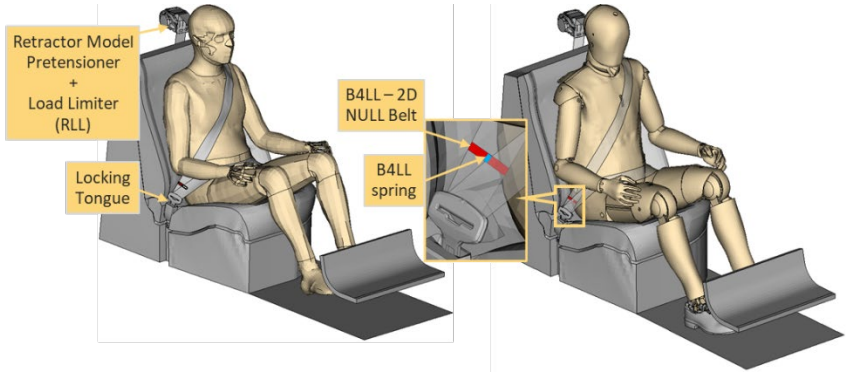

Fig. 1 (a). Set-up with the B4LL spring model: SAFER HBM (left) and THOR (right) in the rear-seat environment.

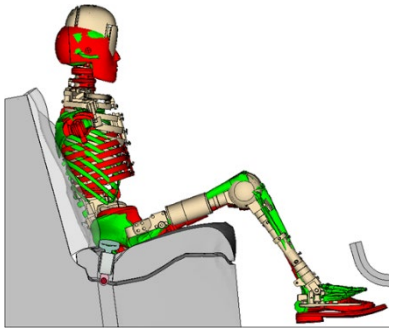

Fig. 1(b). Overlaid skeletal of H350 (red), SAFER-HBM (green) and THOR (wheat).

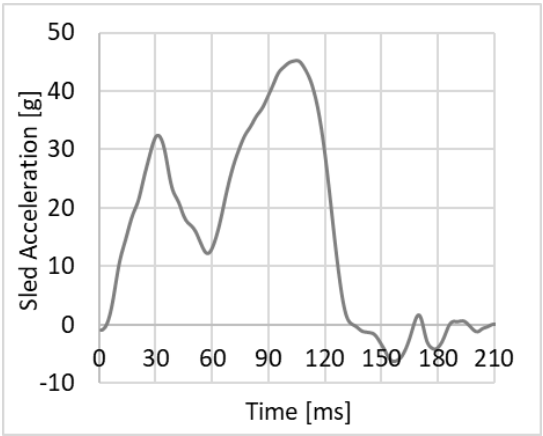

Fig. 2. Crash pulse utilized in the simulations.

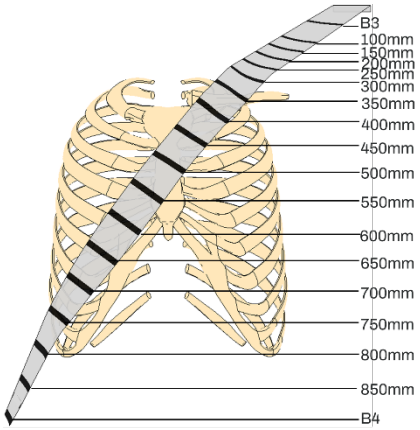

Fig. 3. Location of sections to calculate belt forces.

The reference belt system consisted of a retractor model, including a pretensioner and a constant force load limiter (called RLL), and a locking tongue. This reference belt system represents advanced belt systems available for the rear-seat occupants in modern vehicles. The constant force RLL level was modeled at 5 kN. This RLL level

falls within the range of recently reported diagonal belt force between 4 kN and 8 kN in the vehicle (average model year 2014) tested in frontal offset configuration at 48 kph [19].

In the variation from the reference case, an additional load limiter (called B4LL) was created at the lower inboard part of the diagonal belt. Therefore, the diagonal belt model was separated into two parts on either side of a row of two-dimensional belt elements across the width (marked in red in Fig. 1(a)), about 60 mm from the locking tongue. The separated belt parts were connected via a spring which controlled the force in the lower diagonal belt. The spring was defined with a constant force-displacement characteristic. The row of belt elements between the two seat-belt parts was retained in the model to maintain the contact between belt and dummy. However, these elements were assigned with null material properties, so they did not contribute to the spring force. The force level in the spring was varied from 3 kN to 5 kN at every 0.5 kN, and simulations were performed to study the effects of B4LL force level.

In all the simulated cases, the pretensioner was triggered at 15 ms after the onset of crash pulse. The locking tongue was locked at the end of the pretensioner stroke (i.e. 30 ms after the onset of crash) to prevent any movement of webbing through the tongue for the rest of the simulation. This was done to ensure that the pelvis coupling remained consistent across the simulations. The friction values for all the contacts were retained from the original validated model. Therefore, the contact between occupant model and seat was defined with a coefficient of friction of 0.5, whereas the contact between the occupant model and the belt was assigned a value of 0.3. In real-life crashes the occupant's clothing can affect the friction between the seat-belt webbing and the occupant, therefore the sensitivity of friction coefficient defined in the contact between occupant model and belt was also studied.

Results Analysis

To quantify the effects of B4LL, simulation results for the reference case and for different variations in B4LL were compared for each occupant model. Simulation responses were evaluated in terms of forces distribution at different belt sections, chest deformation, and forward excursion at head, chest and pelvis to achieve a reliable comparison. Belt force was evaluated at every 50 mm on the diagonal belt. Therefore, 18 sections were defined on the belt. Their respective locations on the belt are illustrated in Fig. 3. For calculating the forward excursion, predefined markers in the occupant models for head centre of gravity (CoG), T4 (for chest), and pelvis CoG were utilized. Chest deformation was estimated differently in both the occupant models. In SAFER HBM, maximum principal strain in all the cortical bone elements in each rib was computed across the simulation duration. The peak strain was then calculated for each rib. Therefore, 24 peak strain values (for 12 ribs in each side) were obtained for each simulation. In THOR, displacement in four chest Infra-Red Telescoping Rods for the Assessment of Chest Compression (IRTRACC), resulting Rmax (maximum displacement out of four IRTRACCs) and Principal Component score (PC score calculated based on [20]) were evaluated. The RLL and B4LL spring deformations were also measured to determine the B4LL design requirements.

A CORA-based colour-gradient-map of correlation values for each section force relative to B3 and B4 was created on the diagonal belt. This visualization showed how the belt force distribution was affected between reference and B4LL cases. It also helped in evaluating the sensitivity of B4LL variations on the diagonal belt. The mapping process is explained below. A detailed exemplary calculation is provided in Appendix A2.

The mapping process is divided into three steps, as illustrated in Fig. 4. In step#1, CORA correlation values were calculated for each section force with respect to the section forces at B3 and B4. Therefore, a pair of correlation values (CORA against B3 and CORA against B4) was calculated for each section. With the correlation values, it can be objectively categorized whether the force at any section correlated better with either B3 or with B4. Obviously, the maximum correlation value of 1.0 was calculated between the same reference sections, i.e. between B3 and B3 and between B4 and B4.

In step#2, the correlation values obtained for a simulation were transformed into a Red, Green and Blue (i.e. RGB) colour gradient. Maximum correlation of 1.0 at section B3 was represented by red colour (i.e. 255, 0 ,0) and at section B4 it was represented by blue colour (i.e. 0, 0, 255). The correlation value calculated between B3 and B4 section forces in the reference case was assumed to represent the zero for both R and B values. Based on this, a colour gradient equation was formulated (given in Fig. 4) for calculating the R and B values for a given section with its correlation pair values. This eventually means that the R and the B values diminish gradually from the highest, at 255, to the lowest, at zero, while moving from their respective end to the opposite end of the diagonal belt.

In step#3, the peak force difference at a given section in a B4LL simulation relative to the reference was represented in the colour-gradient-map. For that, the ratio of peak forces for the matched section between a B4LL simulation to reference was transformed into transparency gradient. The highest value of force ratio (i.e. 1.0) was represented by full opacity (i.e. 255) and the lowest as full transparency (i.e. 0). Based on this, a transparency gradient equation (given in Fig. 4) was formulated to calculate the transparency value (named as Tr) for a given section in a simulation relative to the reference. This indicates that reference simulation achieved the highest opacity (i.e. 255). Eventually, a set of R, B and Tr values for each section was calculated and used to colour the set of belt elements from one section to the next section. There was no averaging used to smooth out the colour differences between the two sections.

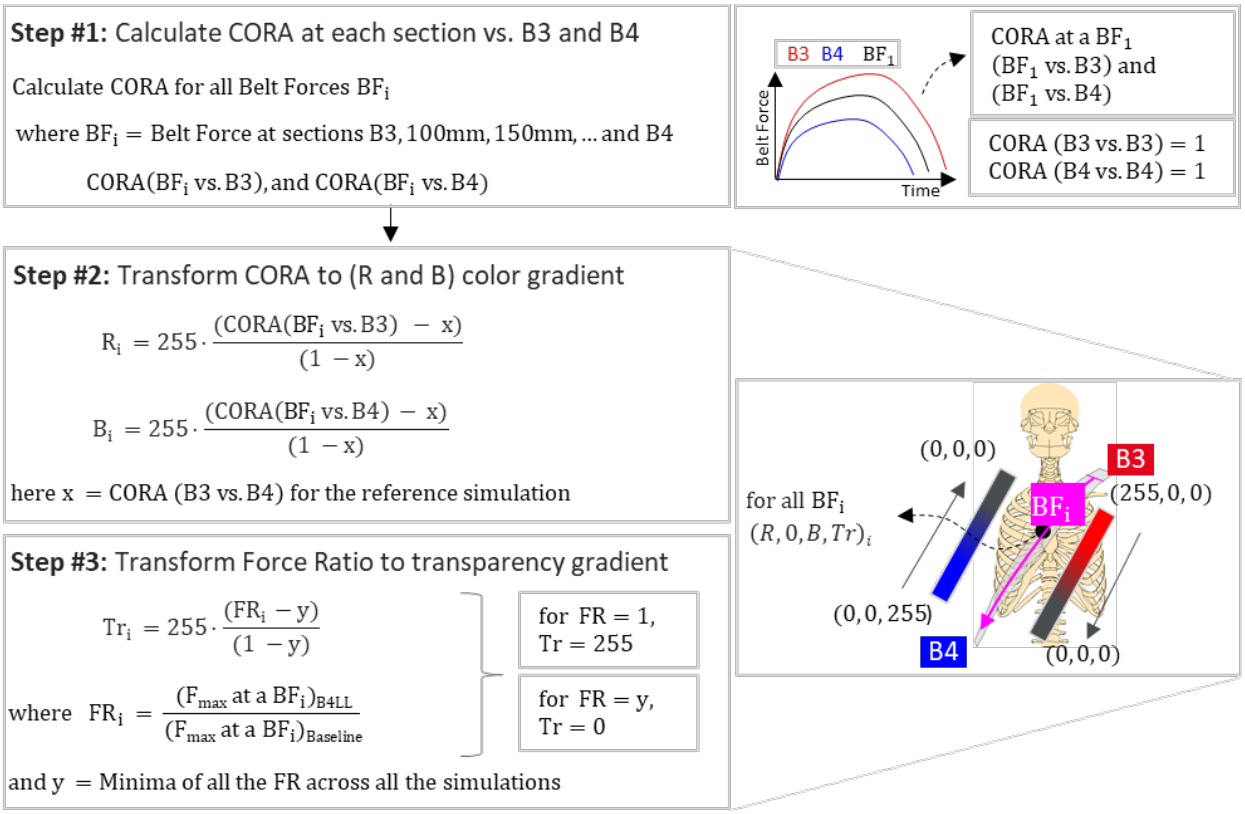

Fig. 4. Creating the CORA-based color-gradient-map for force distribution on the diagonal belt.

III. RESULTS

In all the simulated cases, the belt restrained the occupant models effectively. In the reference simulation, the restraining belt force was controlled by the RLL only, resulting in 337 mm of extension in the RLL spring. In the B4LL simulations, the additional load limiter modelled at the lower inboard belt portion worked in combination with the RLL to share the occupant load and was therefore also stretched. Table 1 gives the peak extension values in RLL and B4LL springs for the simulated cases. For the lowest B4LL level of 3 kN, the B4LL spring extended the most, by 70 mm, resulting in about 40 mm less extension in the RLL spring (i.e. at 298 mm) from its reference value.

TABLE I
PEAK EXTENSION VALUES IN RLL AND B4LL SPRINGS

Simulated Case	RLL Spring Extension (in mm)	B4LL Spring Extension (in mm)
Reference	337	--
B4LL 5.0 kN	337	0
B4LL 4.5 kN	336	9
B4LL 4.0 kN	331	20
B4LL 3.5 kN	326	40
B4LL 3.0 kN	298	70

Effects of B4LL on the Diagonal Belt Force Distribution

Figure 5 and Fig. 6 compare the peak force at different belt sections between reference and various B4LL simulated cases with SAFER HBM and THOR, respectively. The belt force time histories for all the cases with SAFER HBM and THOR are plotted in Appendix A3 (a) and (b), respectively.

Irrespective of the occupant models, the RLL controlled the force in the upper shoulder belt in all the simulated cases, and thus the B3 section force always reached the RLL level of 5 kN. The peak belt force stayed at 5 kN until the section at 300mm, then gradually reduced till the section at 550mm and increased thereafter. In the reference cases, force at the B4 section was likewise as high as 5 kN. However, inclusion of the B4LL enabled the force in the lower part of the belt to be restricted to the simulated B4LL level. For the highest level of B4LL at 5 kN, the B4 force was close to the reference (i.e. 5 kN), but it gradually decreased with the decreasing B4LL levels, eventually producing the lowest B4 force with the lowest level of B4LL at 3 kN.

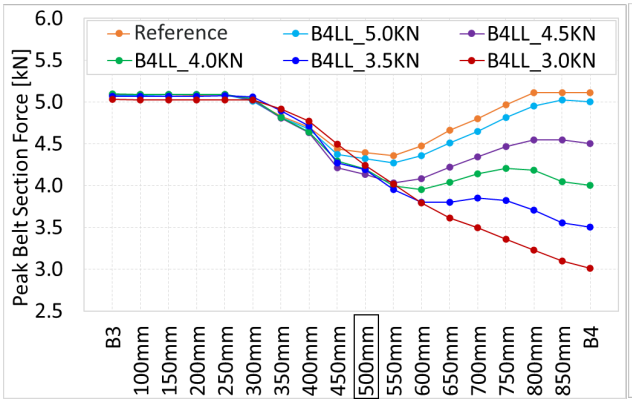

Fig. 5. Peak belt forces at different sections between Reference and B4LL cases from SAFER HBM simulations (marked belt section at 500 mm is at mid-sternum).

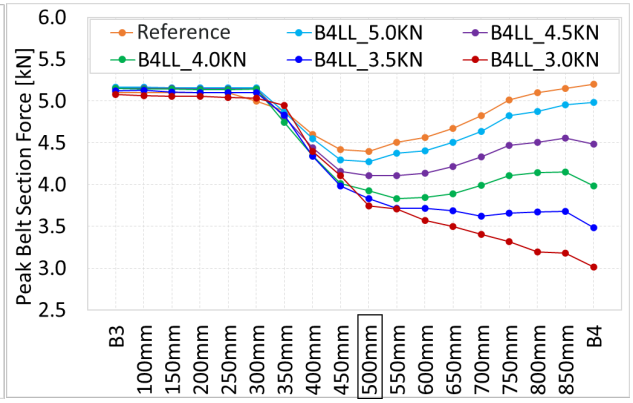

Fig. 6. Peak belt forces at different sections between Reference and B4LL cases from THOR simulations (marked belt section at 500 mm is at mid-sternum).

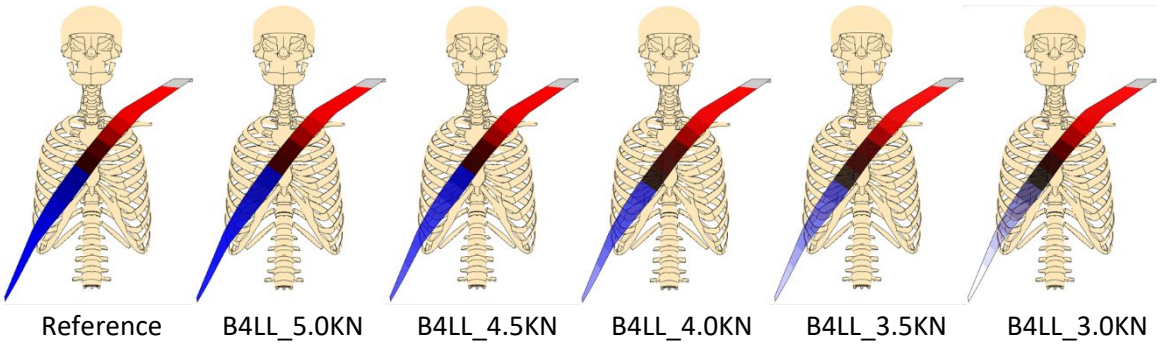

Fig. 7. Colour-gradient-map on the diagonal belt for CORA-based correlation of section forces with respect to the force at the B3 and at the B4 for SAFER HBM simulations.

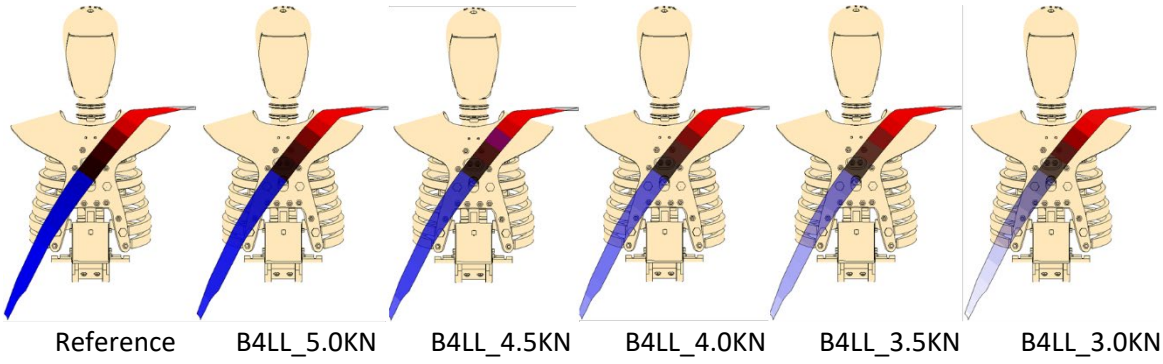

Fig. 8. Colour-gradient-map on the diagonal belt for CORA-based correlation of section forces with respect to the force at the B3 and at the B4 for THOR simulations.

Figure 7 and Fig. 8 show colour-gradient-map on the diagonal belt for simulations with SAFER HBM and THOR, respectively. Based on the correlation with either B3 (or RLL) or B4 (or B4LL) force, the diagonal belt can be divided into three distinct zones (as shown in Fig. 7 and Fig. 8): the RLL controlled zone from the retractor to the upper

sternum (in colour red); a transition zone in the belt segment across the sternum; and finally the B4LL controlled zone from lower sternum to the locking tongue (in colour blue). The colour distribution did not change in any of the simulated variations, implying that the effectiveness of both the RLL and the B4LL remained confined within their respective controlling zones. The colour transparency level decreased steadily in the blue colour area only, with almost no change in the other belt segments, indicating that the force intensity gradually reduced, primarily in the lower diagonal belt, as the B4LL levels dropped from the highest level at 5 kN to the lowest level at 3 kN.

The B4LL effective zone (in blue colour) extended further up to the mid-sternum region with THOR (Fig. 8), resulting in a shift in the transition zone on the upper chest region rather than across the sternum, as shown in the SAFER HBM (in Fig. 7). Other findings from the SAFER HBM were directly applicable to the THOR.

Effects of B4LL on the Chest Loading

Figure 9 shows the peak strains in each rib in the SAFER HBM for all the simulations. The inboard side ribs are plotted on the left side of the plot, while the outboard side ribs are plotted on the right side. For all the simulated cases, except in rib R1, the peak strains were consistently higher in the ribs located along the belt path, i.e. upper outboard ribs from L1 to L5 and lower inboard ribs from R5 to R10, indicating clear evidence of belt-induced chest loading. Moreover, the inboard ribs experienced higher strain in comparison to the outboard ribs, and rib R8 was the most strained, followed by R7, R9 and R6. The high peak strain in rib R1 was unexpected, mainly because it was not directly loaded by the belt. Rib R1 was therefore excluded from further analysis.

The strain in the ribs was the highest in the reference (the highest at 3.85% in R8, followed by 3.66% in R7, 3.27% in R9, 2.91% in R6 and 1.97% in L3), which reduced when B4LL was applied (as shown in Fig. 9). The higher levels of B4LL (i.e. 5 kN and 4.5 kN) were only marginally effective; the 3 kN B4LL was very effective. The six most strained ribs in the reference case experienced more than 30% reduction in their peak strain with the 3 kN of B4LL (47% drop in rib R6, 45% drop in rib R9, 41% drop in rib R7, 36% drop in rib R5, 34% drop in rib L5 and 30% drop in rib R8).

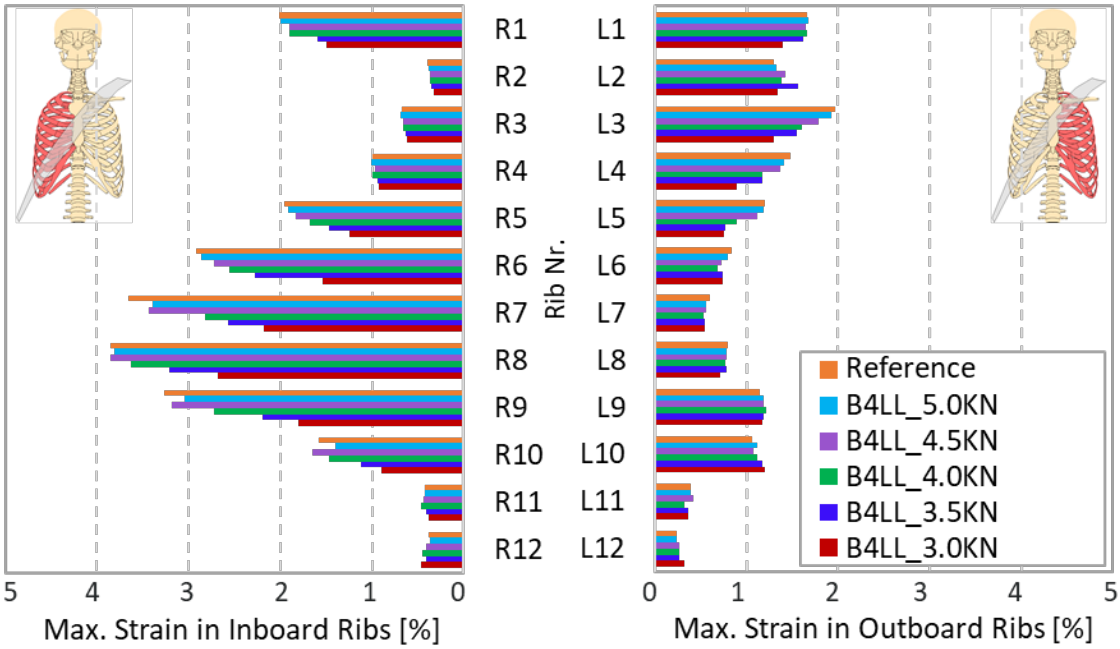

Fig. 9. Peak strains in the ribs in SAFER HBM: comparison between the reference simulation and variations in B4LL.

In any simulated case, displacement in the inboard IRTRACCs was higher (40 mm or more in both the upper and the lower IRTRACCs) than in the outboard IRTRACCs (between 30 mm and 40 mm in the upper and between 20 mm and 30 mm in the lower IRTRACC), see Fig. 10(a). The IRTRACCs displacements were the highest in the reference and reduced when B4LL was applied. The most substantial decline was seen in the lower inboard IRTRACC with the lowest B4LL level at 3 kN: a maximum reduction of 14 mm (i.e. decreased by 27% from 54 mm in reference to 40 mm). However, the drop in the upper inboard IRTRACC displacement was relatively lower: the largest drop was 5 mm with the 3 kN of B4LL.

The Rmax and the PC score (shown in Fig. 10(b)) reflect the reduced chest compression with the B4LL compared

to the reference. However, the Rmax, a global-level chest injury assessment measure, was less sensitive to the change in the B4LL than the individual IRTRACC displacement representing localized chest loading. Based on the peak Rmax values, the 3 kN B4LL achieved the maximum reduction in the chest displacement of 10 mm (i.e. from 54mm to 44 mm) from reference, resulting in a 19% drop, whereas the highest reduction at an individual IRTRACC level was 14 mm (i.e. from 54 mm to 40 mm), resulting in a 27% drop. In addition, the PC score dropped by 14% (i.e. 6.73 from 7.85) for the 3 kN B4LL compared to the reference.

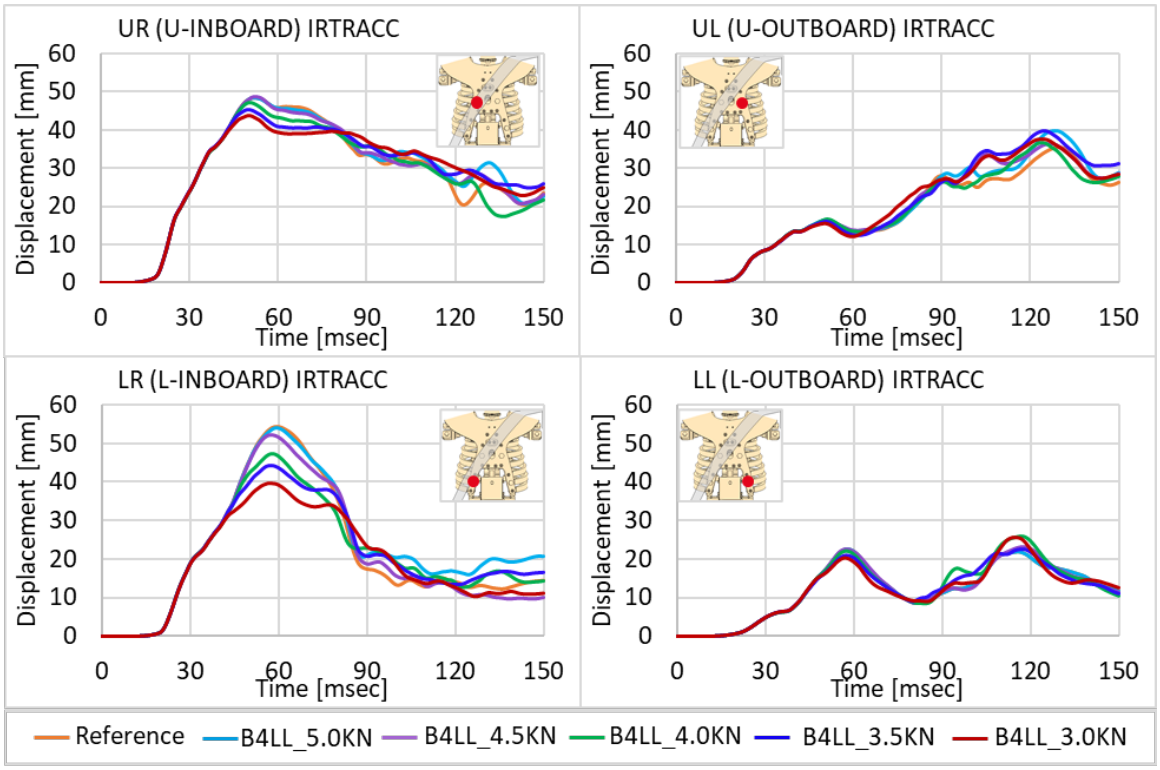

(a)

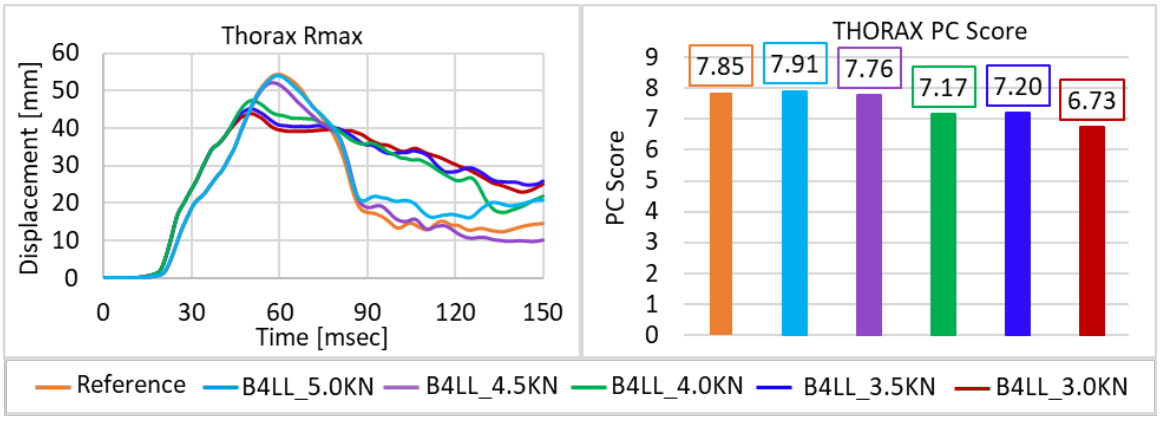

(b)

Fig. 10. Comparison between the reference simulation and variations in B4LL (a) for displacements in four chest IRTRACCs in the THOR and (b) resulting Rmax (left) and PC score (right).

Effects of B4LL on the Forward Excursion

The forward excursion at Head CoG, T4, and Pelvis CoG for SAFER HBM and THOR is shown in Fig. 11. When compared to the reference, the x-displacement at all markers increased the most with 3 kN of B4LL, however the difference remained below 25 mm for both occupant models. The x-displacement of SAFER HBM increased by only 21 mm at Head CoG, 22 mm at T4, and 2 mm at Pelvis CoG with the 3 kN of B4LL compared to their reference values. Similarly, THOR increased its x-displacement by 15 mm at Head CoG, 16 mm at T4, and 5 mm at Pelvis CoG with the 3 kN of B4LL compared to reference values.

Sensitivity of Friction between Belt-to-Occupant model

Sensitivity of the friction between belt-to-occupant model was studied for the reference simulation case with the SAFER HBM model. The two selected values of 0.15 and 1.0 covered the range of friction coefficients reported in reference [21] for different fabric-to-fabric and fabric-to-leather combinations. It was observed that friction coefficient affected both the belt section forces and the resulting peak rib strains (as shown in Fig. A.5 in Appendix A5). However, the margin of variation from the nominal friction case (i.e. 0.3) was less than 10% for both the peak belt section forces and the peak strains in the most critical ribs.

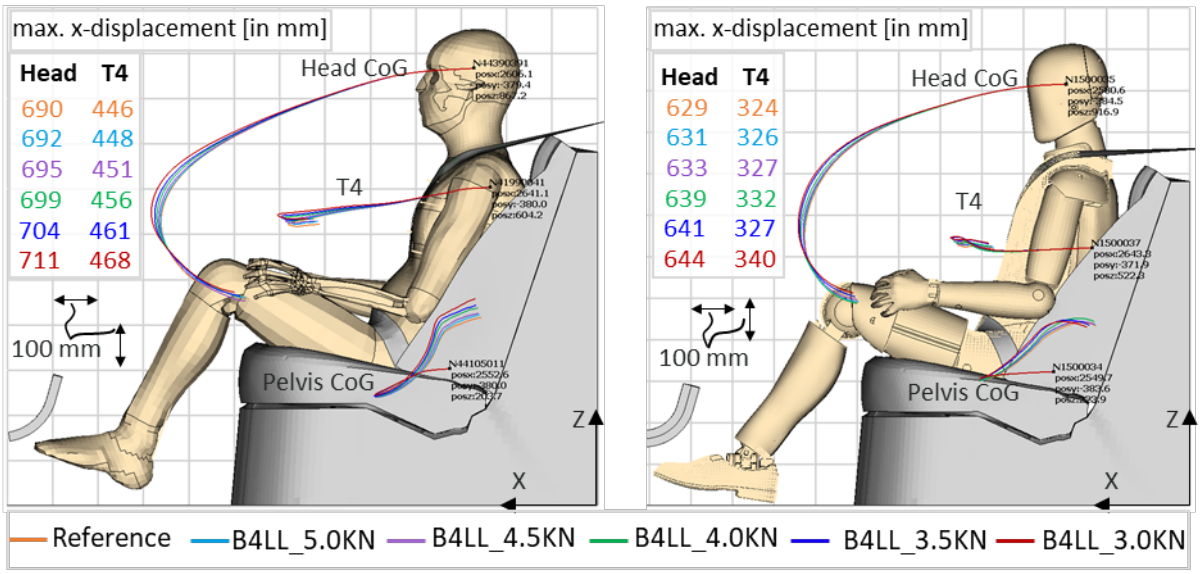

Fig. 11. Comparison of head, chest, and pelvis trajectories relative to sled floor with SAFER HBM (left) and THOR (right), including maximum displacement of head CoG and T4 in x-direction.

IV. DISCUSSION

The potential of an additional load limiter at the lower diagonal belt portion, i.e. B4LL, was investigated with the intention of better controlling the force in the lower inboard belt and thereby reducing the chest deformation, without substantially affecting the forward excursion. A frontal crash at 56 kph was simulated with mid-sized male occupant models of SAFER HBM and THOR on a generic rear seat. A retractor model with a pretensioner and a load limiter (i.e. RLL) at 5 kN level, along with a locking tongue, was used as a reference belt system. Additionally, the B4LL was modeled using a spring with a constant force level varied from 3 kN to 5 kN.

It was observed from the reference simulations with both the occupant models (SAFER HBM and THOR) that, while the force at the upper shoulder belt was limited by the RLL at 5 kN, the force in the lower inboard region of the belt also reached close to 5 kN. As a result, the chest experienced belt-induced concentrated force along the belt path, leading to significant deformation on the inboard side of the chest, indicating an increased risk of rib fracture in the inboard ribs. These findings are consistent with previous laboratory studies [11][13], which reported a direct link between increasing chest deformation to higher force in the lower inboard diagonal belt, as well as with real-life data [16], which indicated that for belted occupants in frontal impacts, fractures were generally confined along the belt path, with a high prevalence of rib fractures on the inboard side of the thorax.

It was found from the B4LL simulations that B4LL allowed to control the force in the inboard belt while not affecting the force in the upper shoulder area. As the occupant restraining force was now shared by both RLL and B4LL, the belt force and the force exerted on the chest were determined by the force level specified at the B4LL relative to the RLL. The lower B4LL levels, from 3.5 kN to 3 kN, were particularly effective in reducing the force in the belt from sternum (by 300 N to 500 N) to locking tongue (1.5 kN to 2 kN) compared to the reference. Consequently, the chest deformation indicators reduced significantly for both SAFER HBM and THOR. There was a maximum reduction of 47% in peak strain value in rib R6 in the SAFER HBM and a 27% reduction in the lower inboard IRTRACC displacement in THOR. This implies that the B4LL and RLL force levels need to be adjusted to achieve an optimum protection for the given crash conditions.

The belt force distribution suggested that each load limiter (i.e. RLL and B4LL) was effective only to a certain distance from its position along the diagonal belt. While the B4LL was effective between locking tongue and the sternum, the RLL was effective from pillar loop to the upper chest area. Furthermore, despite variations in B4LL

force level, the respective area of effectiveness of each load limiter remained almost unchanged. It was observed that B4LL covered a bigger region of the occupant's chest than the RLL.

The RLL effective belt portion, while restraining the occupant's shoulder and upper chest area to prevent the upper torso from rotating forward, better controls the forward excursion than chest deformation. On the other hand, B4LL effective belt portion served as a cushion to relieve pressure on the lower chest while balancing the force with RLL, resulting in better control of the chest deformation than forward excursion. This could explain why, even with the lowest level of B4LL at 3 kN, the occupant forward excursion did not increase considerably (less than 25 mm) when compared to the reference, as the belt force at the upper shoulder remained at 5 kN. Conversely, it might be argued that variation in RLL in the reference model cannot reduce the chest deformation to the level achieved with 3 kN B4LL without significantly increasing the forward excursion. The sensitivity of RLL variation with SAFER HBM showed (in Appendix A4) that when RLL is reduced from 5 kN (reference case) to 3 kN level, it could reduce the rib strains close to B4LL at 3 kN simulation, however it increased the forward displacement by more than 100 mm at the T4 level. This result is consistent with previous studies [8-11], which also reported an increase in forward excursion when the load limiter level at the retractor was reduced.

Based on the results, the initial design target for B4LL can be defined as a force level at 3 kN and webbing pay-out of 70 mm. Both the target force level and the webbing pay-out are feasible to achieve using existing load limiter technology with torsion bars. However, its direct implementation may not be possible without modifying its size. The B4LL is intended to be mounted above the buckle area, where space is often limited. Besides, the metal structure should not increase injury risk due to hard contact. A basic approach of folds sewn on the lower inboard part of the diagonal seat belt could be a simple solution. However, for B4LL to work properly, there must be no webbing slippage through the locking tongue during the load-limiting phase. While a time-based sensor was used to effectively lock the webbing slippage in simulations, a state-of-the-art belt separation tongue that separates shoulder and lap belt portions would be required in hardware instead of a locking tongue.

The efficacy of B4LL in reducing the chest injuries for rear-seat occupants can be compared to at least two other technical options reported in the literature: 1) a lap-belt load limiter [22]; and 2) airbags for rear-seat [12]. The lap-belt load limiter can be installed either side of the lap belt, i.e. at the end bracket side and at the buckle side, and hence offers various configurations. A lap-belt load limiter at the buckle side only is the relevant configuration to compare with the B4LL. In contrast to the B4LL, the lap-belt load limiter is mounted below the buckle assembly and thus has advantage over B4LL in terms of product design and installation. However, it was reported from a simulation study with SAFER HBM [22] that the buckle-only configuration of the lap-belt load limiter reduced forces on the pelvis but increased risk of rib fractures and therefore was not recommended. Instead, a double lap-belt load limiter configuration was shown to be effective in reducing the force to both the pelvis and the thorax, with relatively small effects to the head forward displacement in x-direction.

Airbags together with seat-belt systems are expected to improve occupant protection in rear seats. However, results from a test study [12] with two physical prototypes of airbag concepts with advanced belt systems showed that the force in the lower inboard diagonal belt was still high and that the chest deflection in THOR was not reduced. The B4LL can be particularly beneficial in reducing the force on the chest along with airbags.

There are several limitations in this study. Only one rear-seat environment, with one initial posture of mid-sized occupant models and one crash pulse, was used. According to real-life data [24], rear seats are occupied by a wide range of occupants of various ages and sizes, which is likely to affect energy management requirements for the belt systems. This study needs to be further extended in the future to investigate the effects of B4LL for other occupant sizes for rear-seat application, and for other belt geometries and crash conditions.

Furthermore, despite not being in the belt path and hence not directly loaded by the belt, the peak strain in the inboard side rib R1 was found to be high for all the simulated cases. This necessitates a closer examination of the SAFER HBM's rib modeling and further improvements.

Another limitation is related to the validation of the model for the simulated load case. The H350 positioned in the rear-seat model was validated against the BIW tests, but in the current study the THOR and SAFER HBM models were positioned in the seat model, with most of the model settings carried over from the original model. This could cause systematic deviations in the model. For example, contact friction values taken from the original model could differ in real-life due to occupant clothing. However, the sensitivity analysis with SAFER HBM in the reference case revealed that the effect of friction was within acceptable limits. It is therefore unlikely to have a substantial impact on the overall outcome of this study. Nevertheless, experiments need to be performed in future to test the efficacy of B4LL. For that, a prototype needs to be designed considering the force levels and required webbing pay-out.

While reducing the belt force is essential for preventing the belt-induced chest injuries, this has been commonly achieved by lowering the force level at upper shoulder area at the retractor. In contrast, the current study attempted to investigate the plausibility of reducing the force on the occupant's chest by controlling the force in the lower inboard diagonal belt. The results of this study contribute to a better understanding of the distribution of force in the diagonal belt. It was demonstrated that B4LL could provide an additional control to balance the force distribution in the diagonal belt in such a way that the chest loading was reduced without substantially affecting the forward displacement. This implies that with B4LL, while there is a better chance of getting a higher European New Car Assessment Programme protocol (Euro NCAP) score due to reduced chest deflection, the slightly increased forward displacement is unlikely to result in failing to fulfil the Regulation No 16 of the Economic Commission for Europe of the United Nations (UN/ECE R16) chest displacement requirements.

V. CONCLUSIONS

The belt load limiter (B4LL) reduced the force in the lower area of the diagonal belt, where the effect of the standard force limiter in the retractor was limited. Consequently, the B4LL successfully reduced force applied on the chest and injury measures without substantially increasing the forward displacement. However, physical tests need to be performed to confirm the current findings.

VI. ACKNOWLEDGEMENTS

The authors would like to thank their colleagues Nils Lübbe and Martin Ostling from Autoliv research for providing valuable feedback that helped to improve the content of the paper.

VII. REFERENCES

[1] NHTSA (2004) Lives saved by the federal motor vehicle safety standards and other vehicle safety technologies, 1960-2002", DOT HS 809 833, October 2004.

[2] Kahane, C. (2013) Effectiveness of pretensioners and load limiters for enhancing fatality reduction by seat belts. NHTSA, DOT HS 811 835, November 2013.

[3] Liers, H., Rößler, R., and Ziegler, J. (2017) Performance of restraint systems in accident – does every occupant benefit equally from the measures? International Technical Conference on the Enhanced Safety of Vehicles, Paper Number 17-0262, 2017.

[4] Kuppa, S., Saunders, J., and Fessahaie, O. (2005) Rear seat occupant protection in frontal crashes. International Technical Conference on the Enhanced Safety of Vehicles, Paper Number 05-0212, 2005.

[5] Jermakian, J., Edwards, M., Fein, S., and Maltese, M. R. (2019) Factors contributing to serious and fatal injuries in belted rear seat occupants in frontal crashes. *Traffic Injury Prevention*, **20**(sup1): S84-S91.

[6] Parenteau, C., and Viano, D. C. (2003) Field data analysis of rear occupant injuries part I: adults and teenagers. Society of Automotive Engineers, 2003.

[7] Brumbelow, M. L., Baker, B. C., and Nolan, J. M. (2007) Effects of seat belt load limiters on driver fatalities in frontal crashes of passenger cars. International Technical Conference on the Enhanced Safety of Vehicles, Paper Number 07-0067, 2007.

[8] Khim, J., Son, C., *et al*. (2013) A study of the relationship between seatbelt system and occupant injury in rear seat based on EuroNCAP frontal impact. International Technical Conference on the Enhanced Safety of Vehicles, Paper Number 13-0153, 2013.

[9] Zellmer, H., Luhrs, S., and Bruggeman, K. (1998) Optimized restraint systems for rear seat passengers. International Technical Conference on the Enhanced Safety of Vehicles, Paper Number 98-S1-W-23, 1998.

[10] Kent, R., Forman, J., Parent, D., and Kuppa, S. (2007) Rear seat occupant protection in frontal crashes and its feasibility. International Technical Conference on the Enhanced Safety of Vehicles, Paper Number 07-0386-O, 2007.

[11] Forman, J., Michaelson, J., Kent, R., Kuppa, S., and Bostrom, O. (2008) Occupant restraint in the rear seat: ATD responses to standard and pre-tensioning, force-limiting belt restraints. *Annals of Advances in Automotive Medicine*, **52**: pp.141–154.

[12] Hu, J., Reed, M. P., *et al*. (2017) Optimizing seat belt and airbag designs for rear seat occupant protection in frontal crashes. *Stapp Car Crash Journal*, **61**(November 2017): pp.67–100.

[13] Eickhoff, B., Zellmer, H., Forster, E. (2007) The mechanism of belt induced chest deflection: analysis and possibilities for reduction. International Technical Conference on the Enhanced Safety of Vehicles, Paper Number 07-0202, 2007.

[14] Bengt, P., Lopez-Valdes, F. J., Lundgren, C., Bråse, D., and Sunnevång, C. (2015) Innovative seat belt system for reduced chest deflection. International Technical Conference on the Enhanced Safety of Vehicles, Paper Number 15-0371, 2015.

[15] Lopez-Valdes, F. J., and Juste-Lorente, O. (2015) Innovative restraints to prevent chest injuries in frontal impacts. International Technical Conference on the Enhanced Safety of Vehicles, Paper Number 15-0381, 2015.

[16] Lee, E. L., Craig, M., and Scarboro, M. (2015) Real-world rib fracture patterns in frontal crashes in different restraint conditions. *Traffic Injury Prevention*, **16**(sup2): S115-S123.

[17] ISO/TS 18571:2014: Road vehicles — Objective rating metric for non-ambiguous signals.

[18] User Manual SAFER HBM v9.

[19] Kathy, T., Suzanne, T., and Alain, B. (2021) Responses of the Hybrid III 5th percentile ATD tested outside of regulatory protocols. International IRCOBI Conference on the Biomechanics of Injury, Paper Number IRC-21-25, 2021.

[20] Poplin, G. S., McMurry, T. L., et al. (2017) Development of thoracic injury risk functions for the THOR ATD. *Accident Analysis & Prevention*, **106**: pp.122–130.

[21] Kothari, V. K., and Ganga, M. K. (1994) Assessment of frictional properties of some woven fabrics. *Indian Journal of Fiber & Textile Research*, **19**: pp.151–155.

[22] Östling, M., and Eriksson, L. (2022) Simulating the Influence of Lap Belt Load Limiting on Injury Risks for Upright and Reclined Occupants with the SAFER Human Body Model. International IRCOBI Conference on the Biomechanics of Injury, Paper Number IRC-22-264, 2022.

[23] Trowbridge, M. J., and Kent, R. (2009) Rear-seat motor vehicle travel in the U.S. using national data to define a population at risk. *American Journal of Preventive Medicine*, **37**(4): pp.321–323.

VIII. APPENDIX

Appendix A1: Summary of validation results

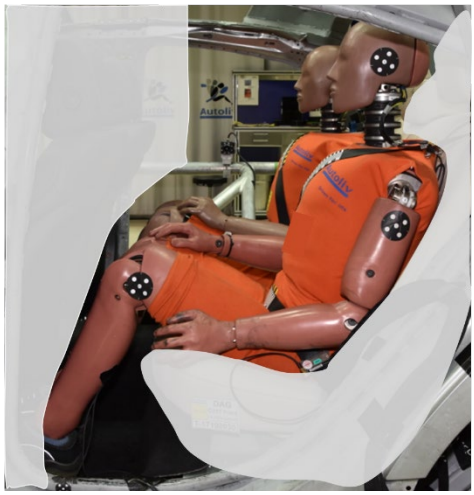

(a) Installation of H350 in the rear seat for a BIW test.

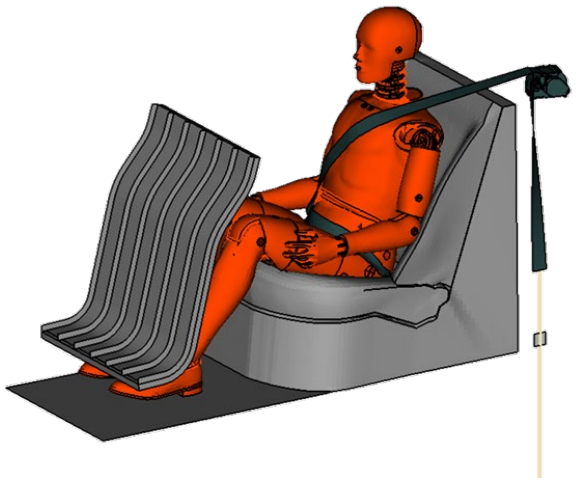

(b) Simulation setup with H350 for model validation.

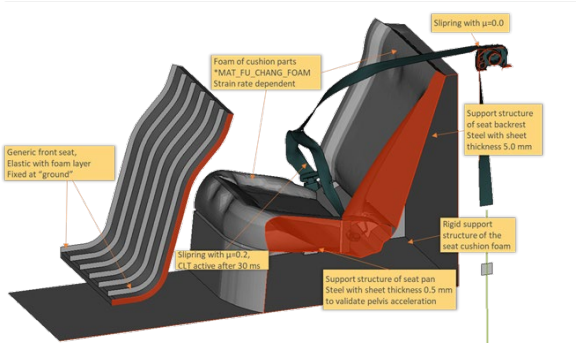

(c) Rear-seat model details.

TABLE AI
COORDINATES OF DUMMY H-POINT AND ANCHORAGES

Location	X	Y	Z
H-point	2426.1	-380.0	200.8
Buckle	2539.3	-146.6	60.5
Anchor	2513.7	-599.0	129.3
Retractor	3064.1	-635.1	691.1

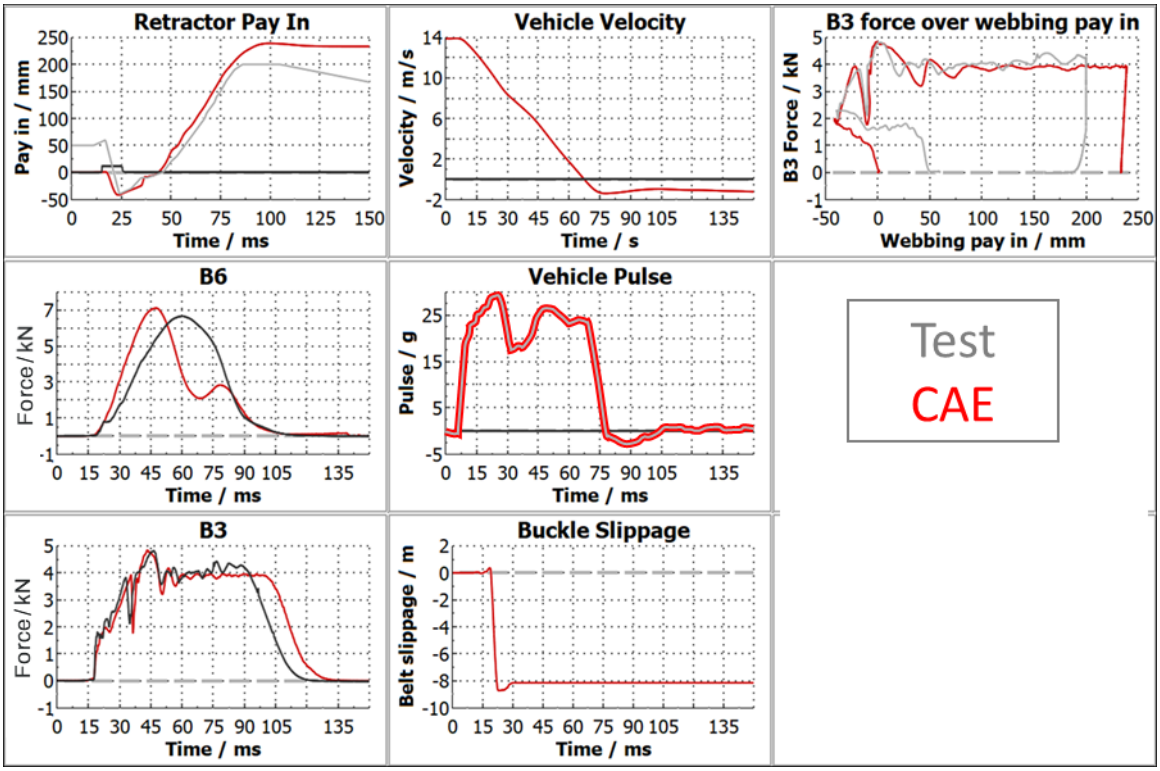

(d) Comparison between test to CAE: Restraint systems outputs.

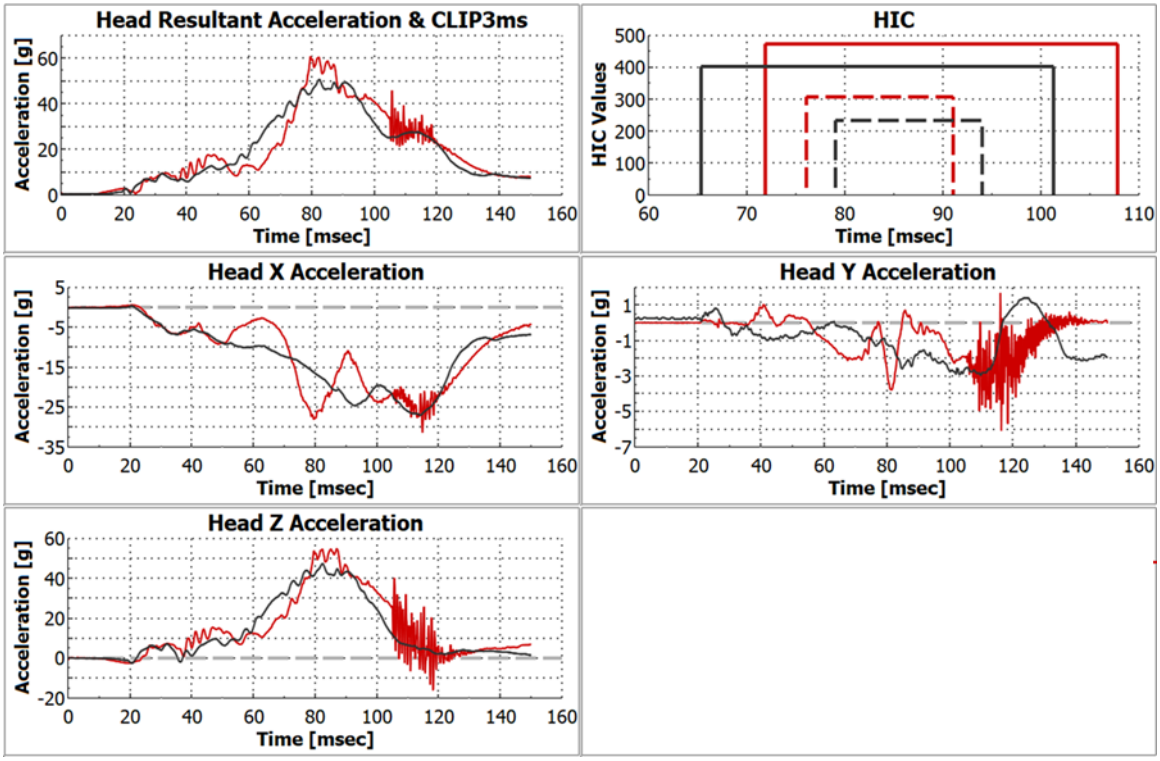

(e) Comparison between test to CAE: Head acceleration and HIC.

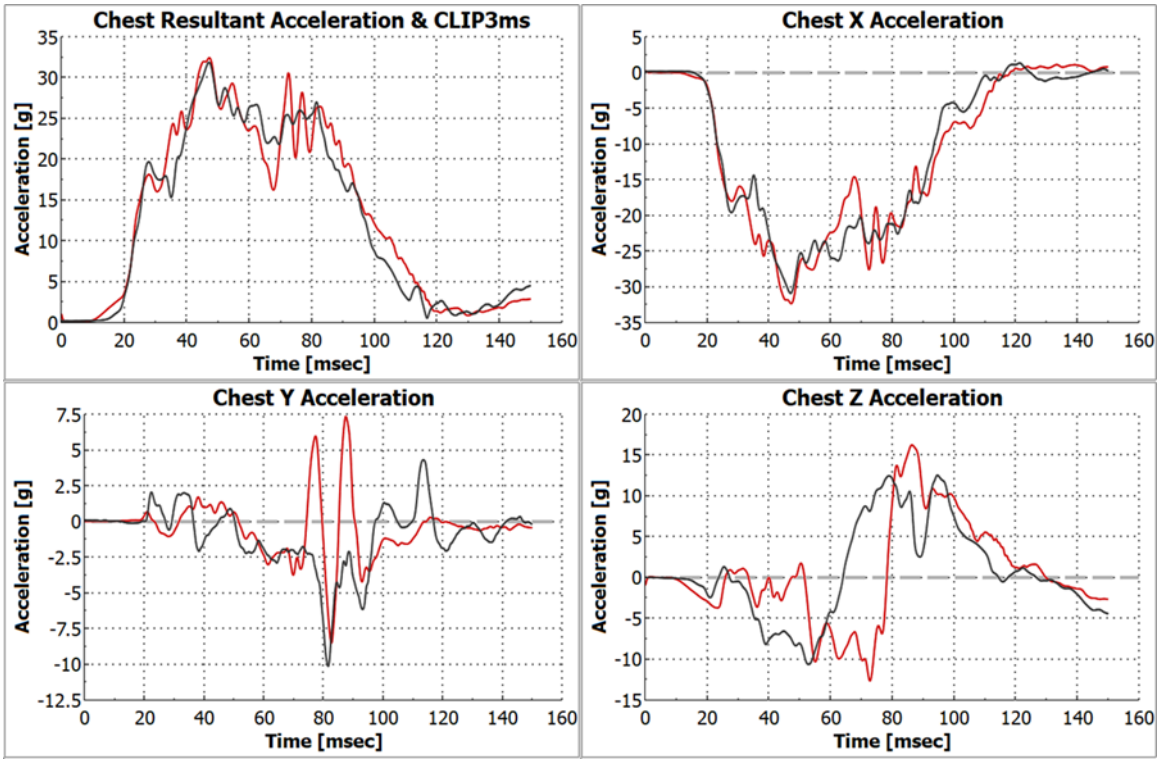

(f) Comparison between test to CAE: Chest acceleration.

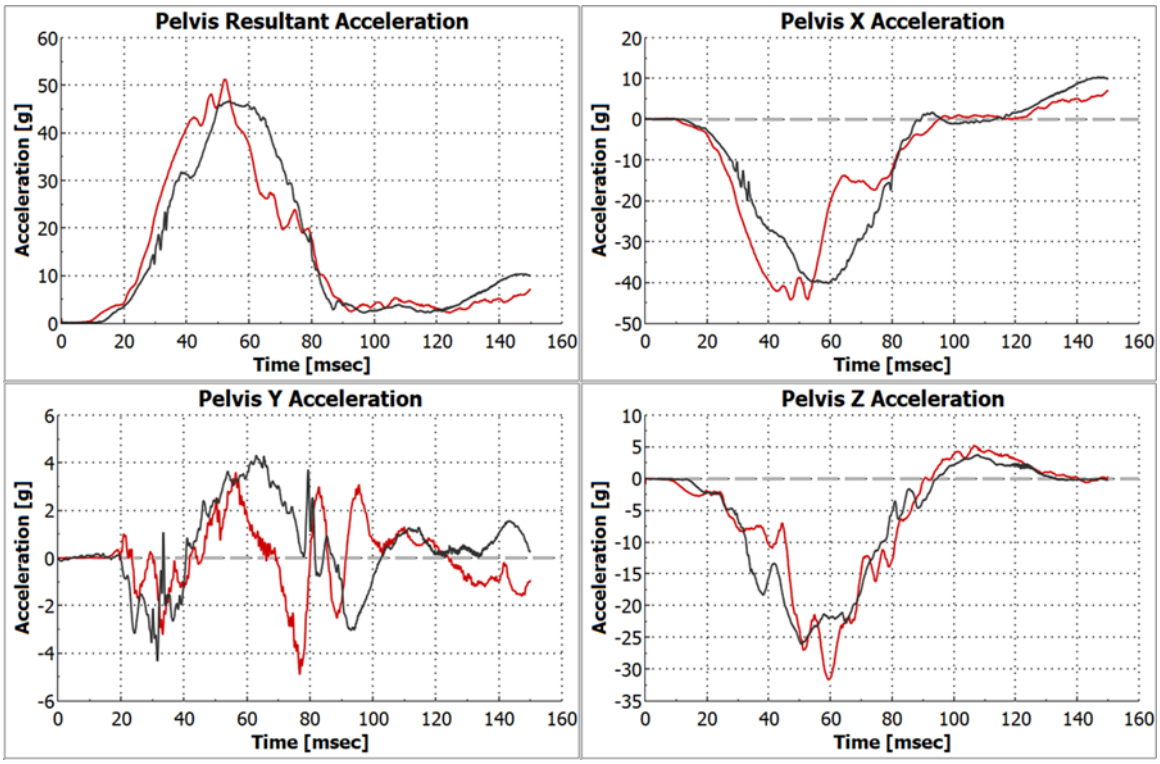

(g) Comparison between test to CAE: Pelvis acceleration.

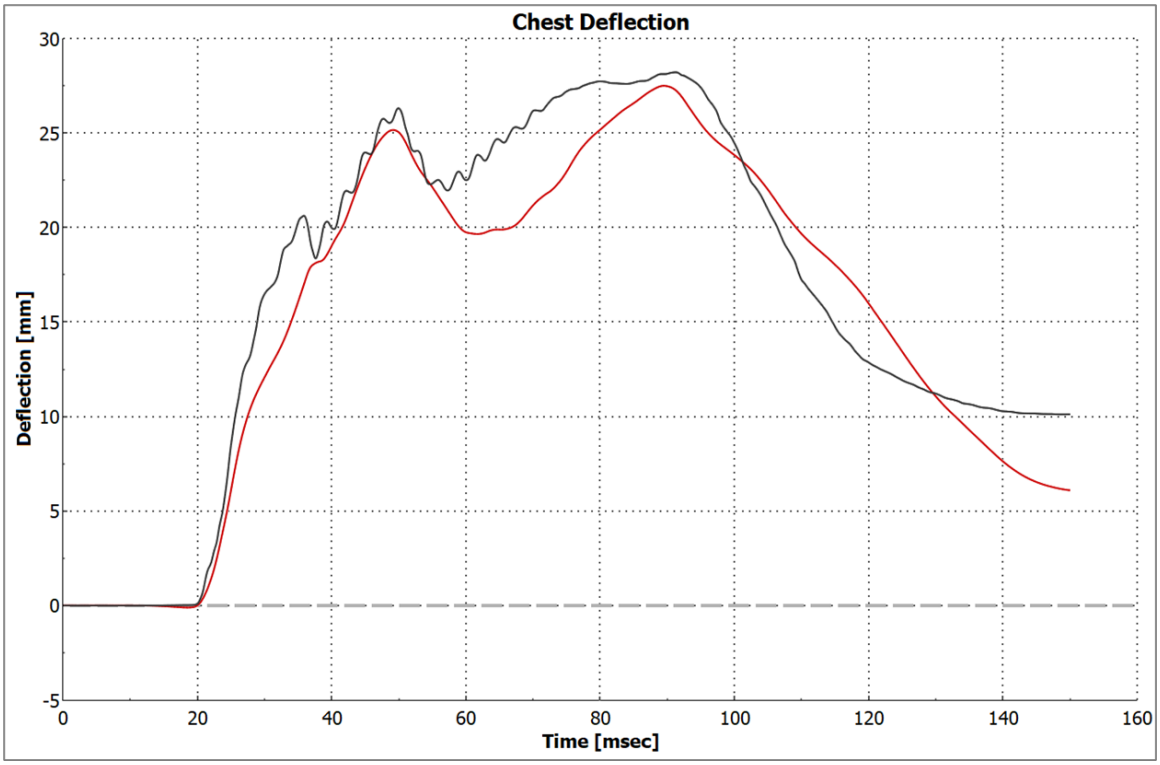

(h) Comparison between test to CAE: Chest deflection.

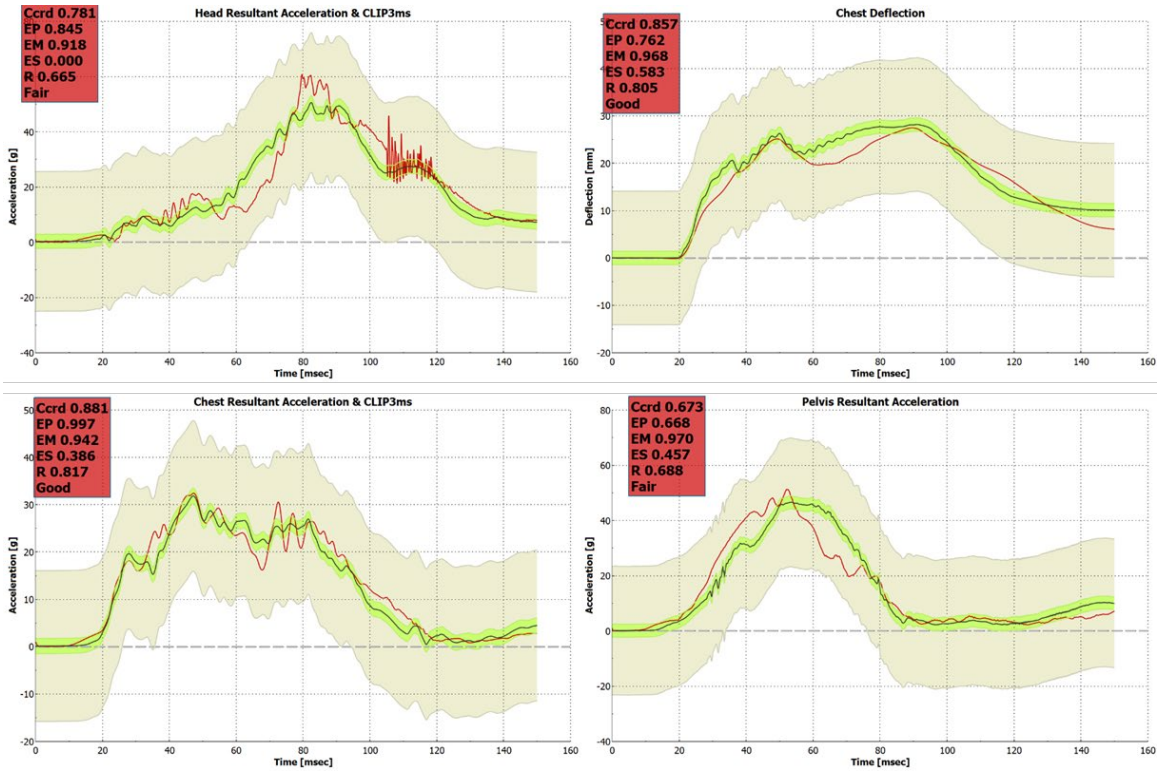

(i) Comparison between test to CAE: CORA rating.

Fig. A.1. Validation summary.

Appendix A2: CORA-based colour-gradient-map: exemplary calculation

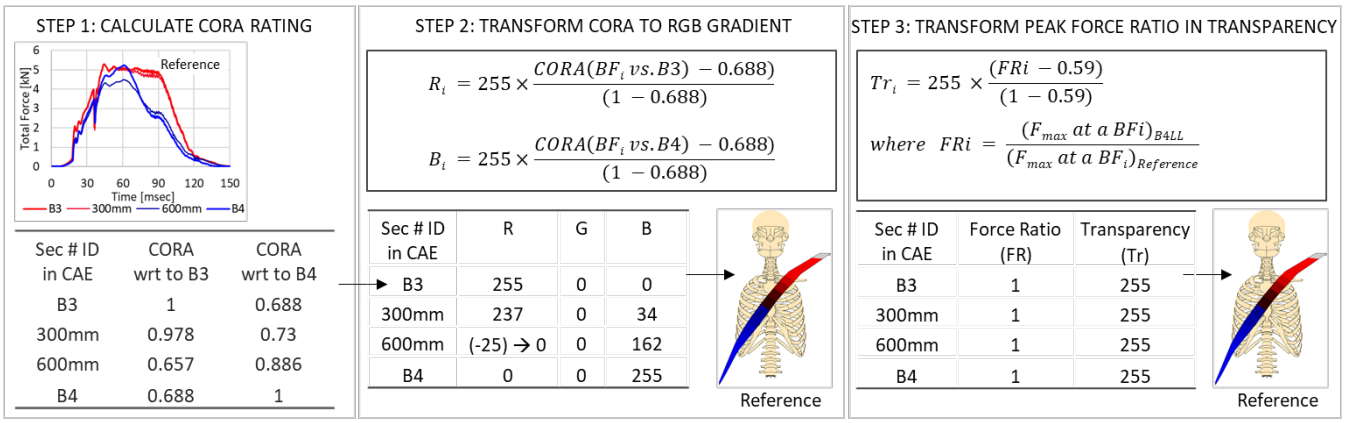

(a) Reference.

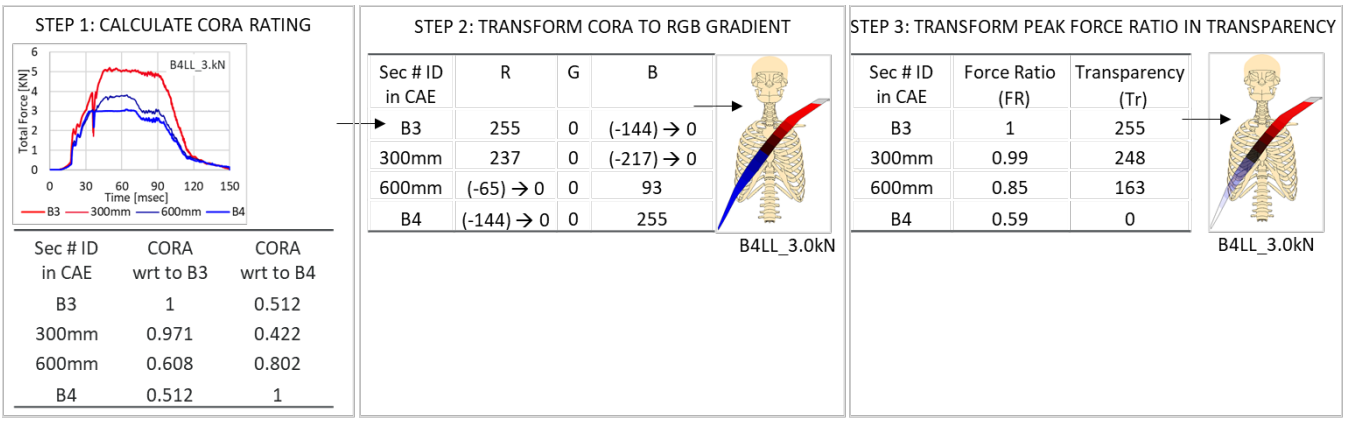

(b) B4LL at 3.0 kN.

Fig. A.2. Flow of calculation for CORA-based colour-gradient-map and transparency applied to (a) reference case and (b) B4LL at 3.0 kN.

Note-1: 0.688 used in Step 2 corresponds to the CORA between B4 and B3 in the reference simulation.

Note-2: 0.59 used in Step 3 corresponds to the minimum of all the FR ratios. It was obtained for B4 section in 3 kN B4LL to the reference.

Appendix A3: Section forces for simulations for SAFER HBM and THOR

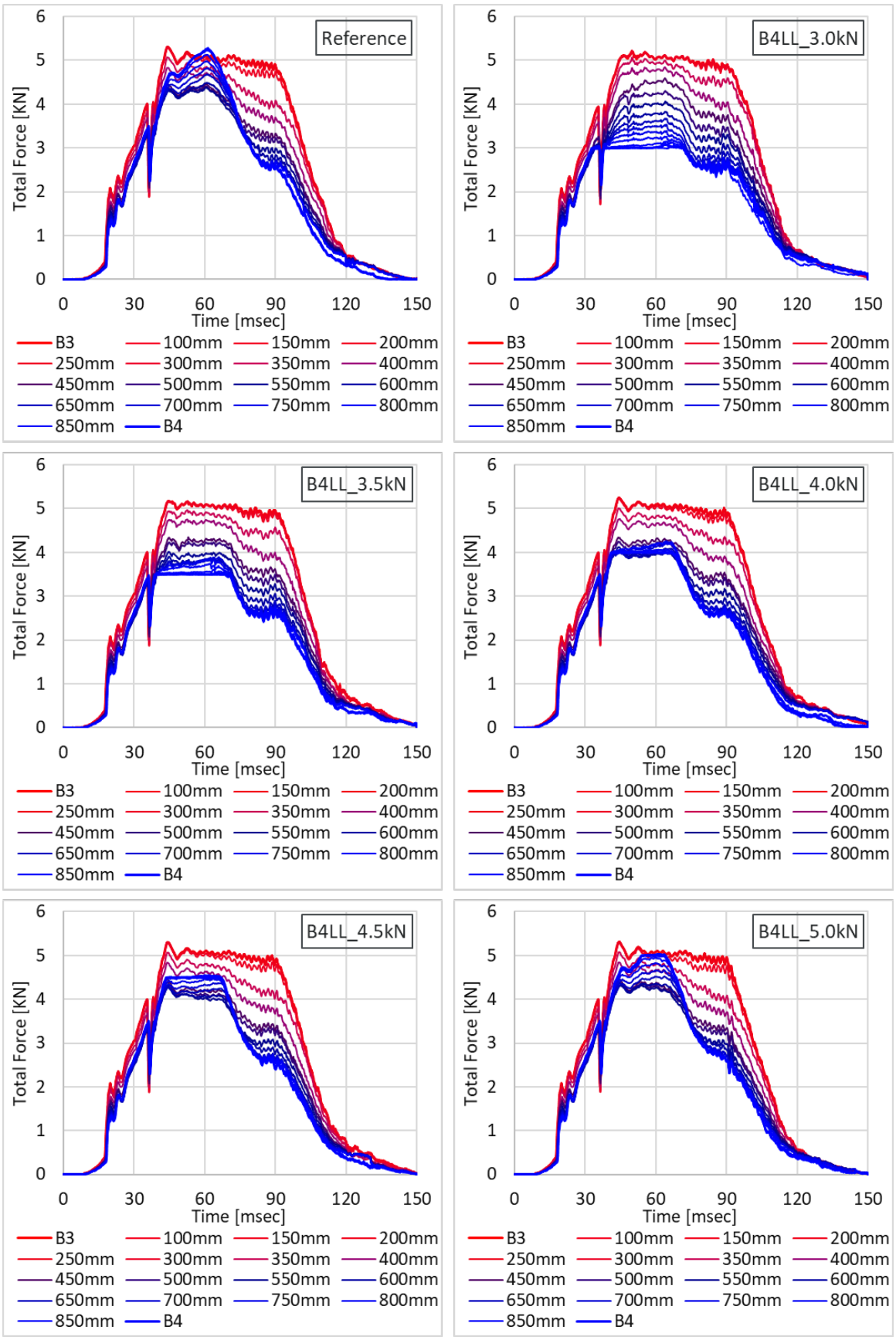

(a)

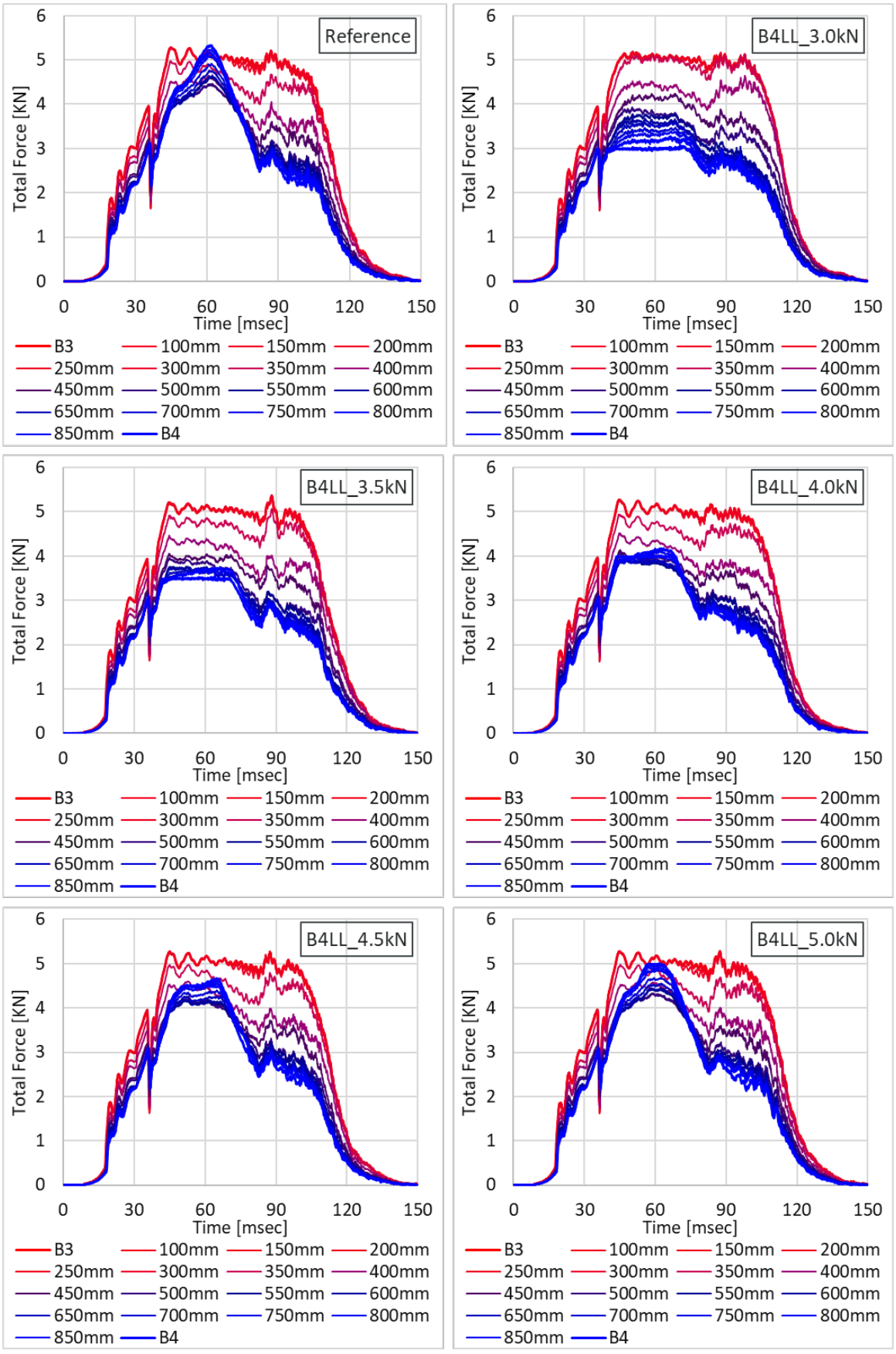

(b)

Fig. A.3. Force in the belt sections for simulations (a) from SAFER HBM and (b) from THOR.

Appendix A4: Sensitivity of Retractor Load Limiter (RLL) simulated with SAFER HBM

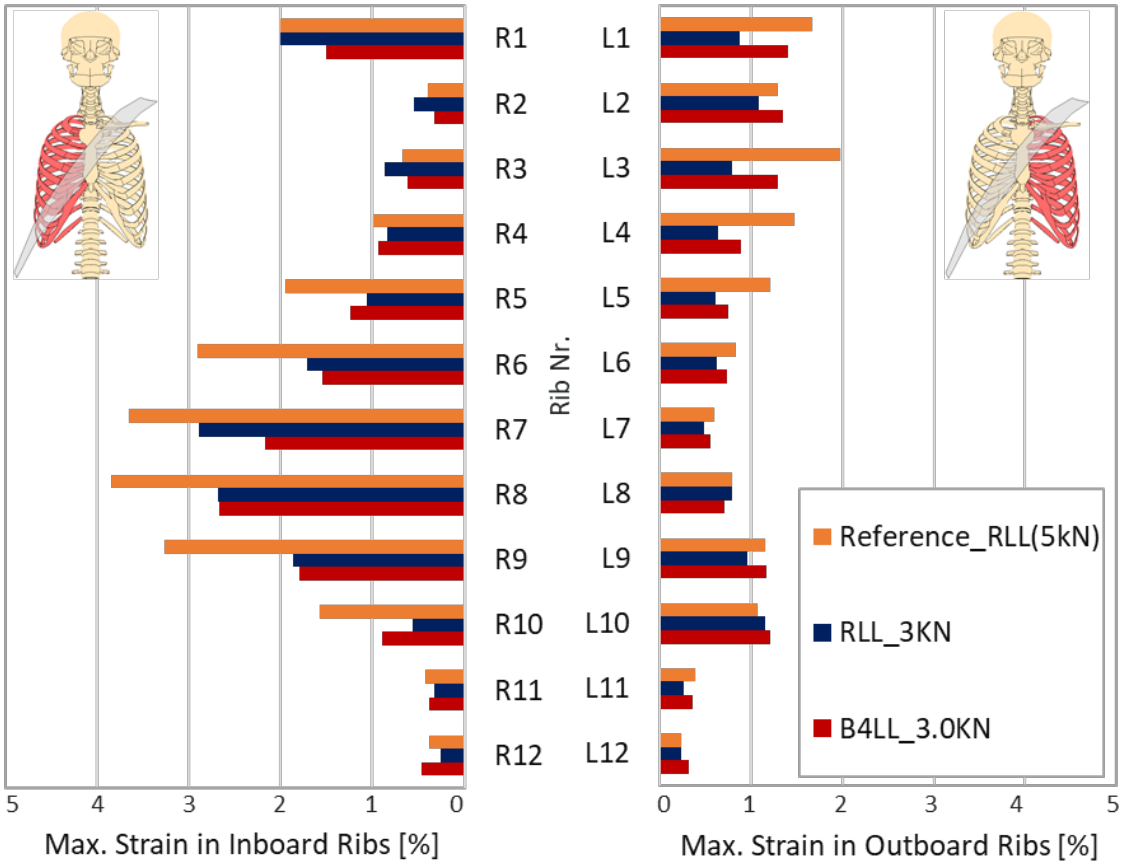

(a)

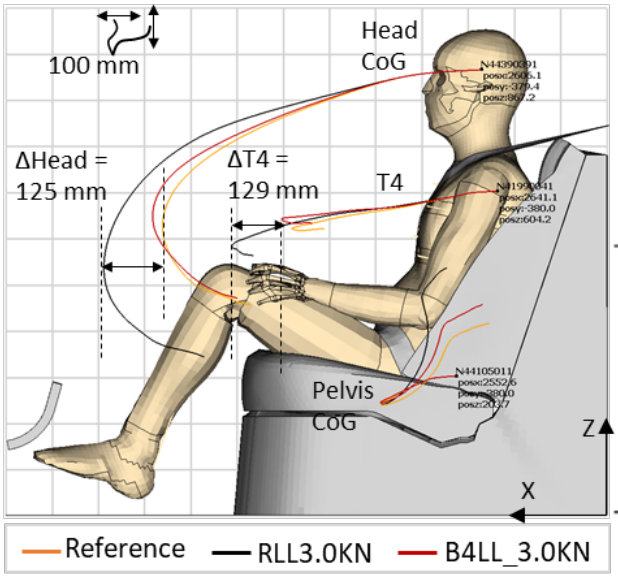

CAE - ID	Head CoG (mm)	T4 (mm)	Pelvis CoG (mm)
Reference	690	446	163
RLL_3.0KN	815	575	164
B4LL_3.0KN	711	468	165

(b)

Fig. A.4. Sensitivity of variation in RLL from reference at 5 kN to 3 kN compared with the lowest level of B4LL at 3 kN (a) peak strains in the ribs in SAFER HBM and (b) head, chest, and pelvis trajectories relative to sled floor (left) and forward excursion in x-direction (right).

Appendix A5: Sensitivity of belt-to-occupant contact friction in reference simulation with SAFER HBM

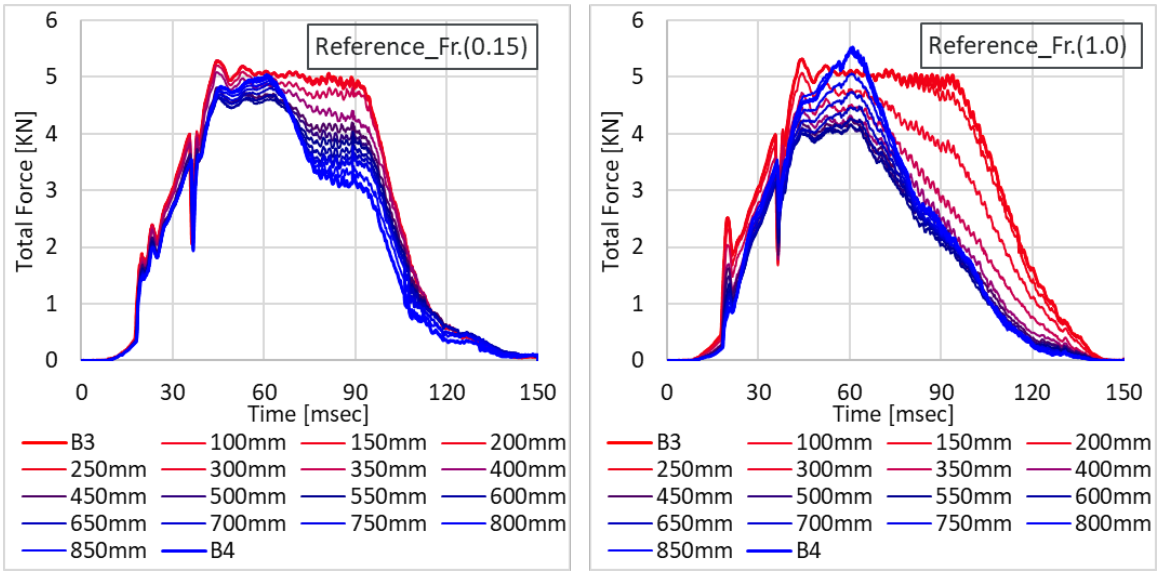

(a)

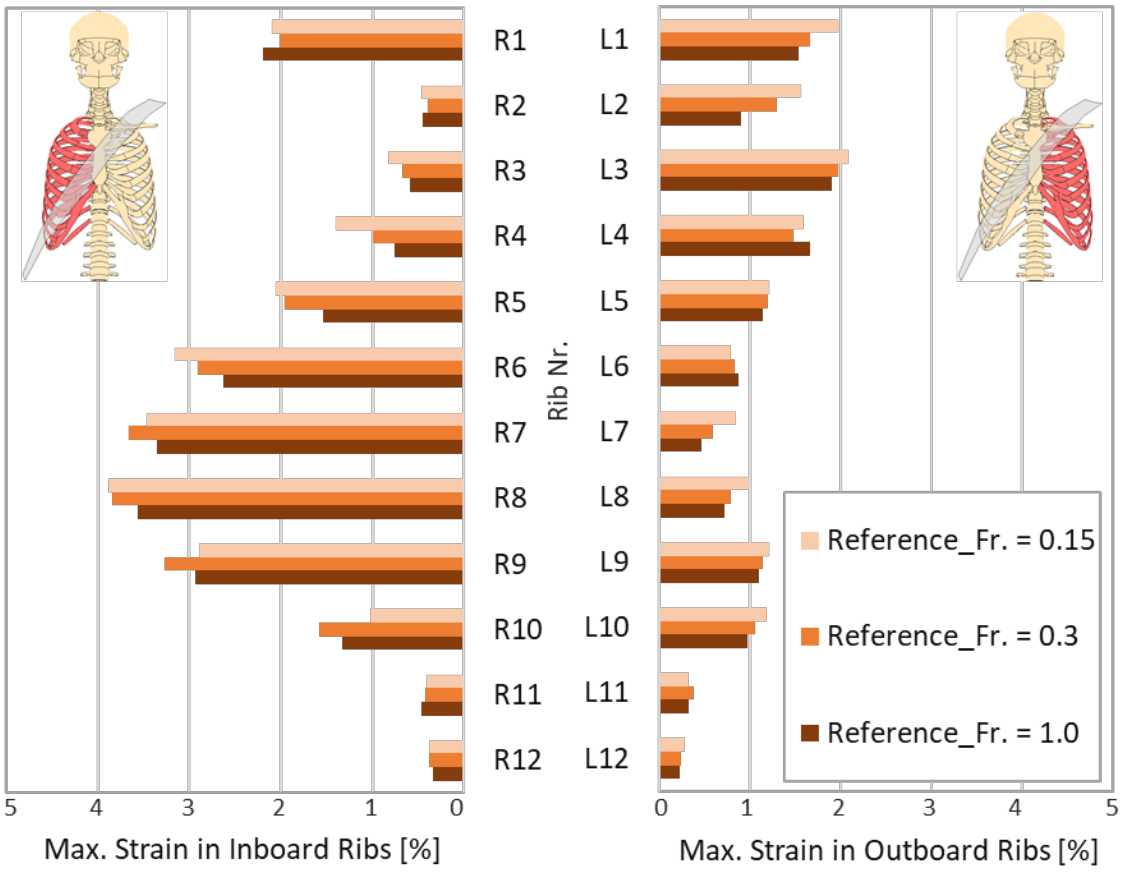

(b)

Fig. A.5. Sensitivity of variation in belt-to-occupant contact friction from its nominal value of 0.3 to a lower value of 0.15 and a higher value of 1.0 in the reference simulation with SAFER HBM on the (a) section forces and (b) peak strains in the ribs.